Amino-functionalized Iron Oxide Nanoparticles Designed for Adsorption of Naphthenic Acids

Galina Simonsen [*], *Mikael Strand, Jens Norrman, Gisle Øye*

Department of Chemical Engineering, Norwegian University of Science and Technology (NTNU), 7491 Trondheim, Norway

ABSTRACT

Amino-functionalized silica-coated iron oxide (Fe_3O_4/SiO_2 NH_2/C_{18}) magnetic nanoparticles were synthesized, and the amino-surface modification was performed by two different methods, a high-pressure autoclave and reflux experiments. The nanoparticles were tested for their ability to remove naphthenic acids from a model crude oil solution and for their magnetic separation properties. Grafting degrees onto the nanoparticle surfaces of 3-aminopropyltrimethoxysilane (APTMS) and n-octadecyltriethoxysilane (ODS) were calculated based on elemental analysis and specific surface area of the nanoparticles was measured by the Brunauer, Emmett and Teller (BET) method. Presence of a core-shell structure of separate nanoparticles as well as nanoparticle agglomerates was confirmed by the use of transmission electron microscopy (TEM) imaging. Average nanoparticle size and coating thickness were calculated based on a TEM size distribution analysis. The two amino-functionalization methods revealed similar results for the adsorption of 4-heptylbenzoic acid (HBA) dissolved in octane, and 2.7 times higher adsorption capacity compared to the unmodified silica-coated (Fe_3O_4/SiO_2) nanoparticles.

Keywords: Magnetic nanoparticles, naphthenate deposits, silica coating, amino-functionalization

1. INTRODUCTION

Production of acidic crude oils has been growing in importance during the past decade. The crude oil acidity is mainly defined by the presence of acidic components or naphthenic acids (NA), which are a complex mixture of cyclic, acyclic, and aromatic carboxylic acids [1, 2]. The presence of these molecules is associated with several problems occurring during crude oil production, such

as corrosion in the refineries [3], pollution of wastewaters [4], formation of emulsions, and calcium naphthenate deposits [5]. The majority of the NA are C10–C50 monoacids with 0–6 fused saturated rings and the carboxylic acid group attached to a ring with a short side chain [6]. In addition, a very small part of them is composed of molecules with four acid functions, named tetra-acids or ARN, often responsible for the formation of calcium naphthenate deposits in the oil fields [7]. The naphthenates are troublesome deposits that can form during crude oil production and processing in systems that handle acidic crude oils with a total acid number (TAN) higher than 0.3 [8]. High TAN crude oils are currently being produced in several regions, such as the North Sea, the Gulf of Mexico, California, Venezuela, West Africa, and China, and is becoming more common, especially in deepwater production. The term "naphthenate deposit" is generally used to describe deposits containing calcium, sodium, magnesium, iron, and other metal naphthenates, and in some cases asphaltenes, scale, and other solids. The naphthenate deposits typically form when naturally occurring NA in the crude oil come in contact with metal ions in the produced water at the right conditions of pH and temperature [9]. It is important to consider oil, water, and the interface between them as a whole system when dealing with problems associated with those acids. Metals can be dissolved in crude oils by formation of complexes with indigenous NA[10]. Being a source of contamination, these metal naphthenates will significantly affect the crude oil quality. The naphthenates are also surface/interfacially active compounds, which tend to accumulate at water/oil interfaces and stabilize emulsions [11]. This will cause operational challenges ranging from oil treating problems and poor water quality to heavy deposits that can plug pipelines and valves [12-15]. The NA and naphthenates can also be present in the water phase causing health and environmental problems [9]. There are several techniques currently used by industry to prevent formation of the naphthenate deposits [9, 16]. One of the most common methods is addition of inorganic, organic, and surfactant acids, which can keep the pH low enough to avoid naphthenate formation. However, the addition of acids is costly, may increase corrosion problems and have a negative impact on the environment. Existing processes for NA removal have varying degrees of success, and there is a need for more efficient and environmentally friendly methods to decrease the NA content and, thus, improve the crude oil quality.

Rapid progress in nanoparticle research have generated an interest to the newly designed materials with properties beneficial for various industries. Among the wide range of nanoscale materials, magnetic nanoparticles represent properties that can be advantageous for applications

in the crude oil production and processing [17-21]. A magnetic nanoparticle is a particle between 1 and 100 nm in size that exhibits magnetic properties when exposed to a magnetic field. Their performance largely depends on the type of material and nanoparticle size. A number of materials can be used for the nanoparticle synthesis, including iron oxides Fe_3O_4, pure metals Fe and Co, spinel type ferromagnets $MgFe_2O_4$, $MnFe_2O_4$, or Co Fe_2O_4 [22]. Chemical stabilization of these particles is usually required as they are easily oxidized in air, resulting in loss of magnetic properties and reduced dispersibility. In many cases stabilization strategies, such as surface coatings with polymers, surfactants, or inorganic compounds, not only protect the particles, but can also be used for further functionalizations [22, 23]. Surface functionalization by introducing specific functional groups is opening for a variety of possible applications. One of the main advantages of this technology is that the magnetic nanoparticles can be recovered at the end of the process by an external magnetic field and potentially reused.

The current work aims to design magnetic iron oxide silica-coated Fe_3O_4/SiO_2 and amino-functionalized Fe_3O_4/SiO_2 NH_2/C_{18} nanoparticles, and evaluate their performance for adsorption of NA from a model oil system. The selectivity towards NA extraction is assessed using commercial non-magnetic amino-functionalized Isolute NH_2 particles and an acidic crude oil from a North Sea oil field. The designed Fe_3O_4/SiO_2 NH_2/C_{18} nanoparticles are obtained through a synthesis by two different methods, a high-pressure autoclave experiment with toluene as a solvent and a reflux experiment with xylene. The silica-coated and amino-functionalized nanoparticles are compared by their efficiency to adsorb the 4-heptylbenzoic acid (HBA) and characterized with respect to various parameters, such as ability to be separated by a magnetic force or magnetic separation, specific surface area, nanoparticle size and thickness of the silica coating as well as chemical composition.

2. MATERIALS AND METHODS

2.1.Synthesis

2.1.1. Materials

A North Sea acidic crude oil was used in this study. The original oil sample was characterized in terms of emulsified water content, density, total acid number (TAN), and asphaltene content. The measured data are presented in Table 1. Aqueous ammonium hydroxide (28-30 %), octane (98 %),

ethanol (96 and 99.8 %), iron (II) chloride (98 %), iron (III) chloride (97 %), hydrochloric acid (37 %), tetraethyl orthosilicate (98 %) (TEOS), 4-heptylbenzoic acid (HBA), aminopropyltrimethoxysilane (97 %) (APTMS), n-octadecyltriethoxysilane (ODS), anyhydrous toluene (99,8 %), anyhydrous xylene (99,8 %), and sodium hydroxide were all reagent grade and purchased from Sigma-Aldrich. All solutions were prepared with ultrapure Milli-Q water (resistivity 18.2 MΩ at 25 °C. Commercial Isolute NH_2 particles with specific surface area of 480 m^2/g and average diameter of 55 μm were purchased from Biotage, Finland. 4-heptylbenzoic acid (HBA) (Fig. 1) dissolved in octane was used as a model oil system.

Table 1. *Physicochemical characteristics of the crude oil*

Characterization parameter	
Emulsified water (wt %)	0.002 ± 0.001
Density (g/cm^3, 20˚C)	0.881 ± 0.001
Asphaltene content (wt %)[a]	0.5 ± 0.02
Total acid number (mg KOH/g)[b]	1.7 ± 0.02

[a] Asphaltene precipitation in n-hexane. Details about method are reported elsewhere [24].
[b] TAN measured according to ASTM D 664-95 standard [25].

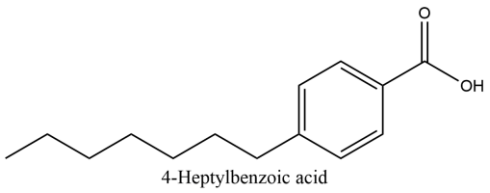

Figure 1*: Structure of 4-heptylbenzoic acid*

2.1.2. Synthesis of Fe_3O_4 nanoparticles by co-precipitation

Iron oxide Fe_3O_4 nanoparticles were synthesized by a co-precipitation method described by Zhang et al. [26]. $FeCl_3$ (20 mL, 1 M, in 0.2 M HCl) and $FeCl_2$ (20 mL, 0.5 M in 0.2 HCl) were mixed and added dropwise within 5 minutes to a stirred solution of sodium hydroxide (1.5 M, 80 °C) contained in a three neck flask with an Allihn condenser. The solution was kept under nitrogen atmosphere while stirred for 20 minutes at 80 °C and subsequently cooled to ambient temperature. The nanoparticles were washed in MilliQ-water and separated by a magnet.

2.1.3. Coating of the Fe_3O_4 nanoparticles with silica

The Fe_3O_4 nanoparticles were coated with silica through a sol-gel approach described by Deng et. al [27]. Fe_3O_4 nanoparticles (0.2 g) were suspended in HCl (100 mL 0.1 M) and kept in an ultra-sonication bath for 25 min. The suspensions were mixed with ethanol (160 mL), Milli-Q water (40 mL) and aqueous ammonia (2.0 mL) in an Erlenmeyer flask. TEOS (0.2 mL) was added under magnetic stirring. The sample was sealed and stirred for 6 hours at room temperature before washing the nanoparticles with a 50/50 water/ethanol mixture several times. The obtained Fe_3O_4/SiO_2 nanoparticles were stored in a water/ethanol suspension. Prior to functionalization, they were dried under nitrogen at 60 °C.

2.1.4. Amino functionalization of Fe_3O_4/SiO_2 nanoparticles

Fe_3O_4/SiO_2 nanoparticles were functionalized with ODS and APTMS in a 1:1 mole ratio by two different methods:

1. According to the procedure described by Zhang et al. [28], the Fe_3O_4/SiO_2 nanoparticles (0.8 g, dried) were dispersed in 80 mL of anhydrous toluene by a 30 min long ultra-sonication. ODS (0.400 mL) and APTMS (0.145 mL) were added under manual stirring and sealed in an autoclave, acid digestion vessel (model 4748 from Parr Instrument). The autoclave was placed in a heating cabinet (120 °C) for 8 hours and then cooled to room temperature. Finally, the nanoparticles were washed and stored in ethanol.
2. A simplified procedure was also developed to functionalize the nanoparticles, where instead of anhydrous toluene, anhydrous xylene (120 °C) in a three neck flask with magnetic stirring and an Allihn condenser was used. The solution was kept in a nitrogen atmosphere, and the obtained nanoparticles were stored in ethanol. The new functionalization method appeared to be easier compared to the autoclave experiment with toluene, which involved high pressure and solvent with lower boiling point.

The overall reaction scheme is illustrated in Figure 2. The ODS and APTMS are shown being grafted onto the silica surface with two anchoring points. In general, the number of anchoring points may vary from one to three.

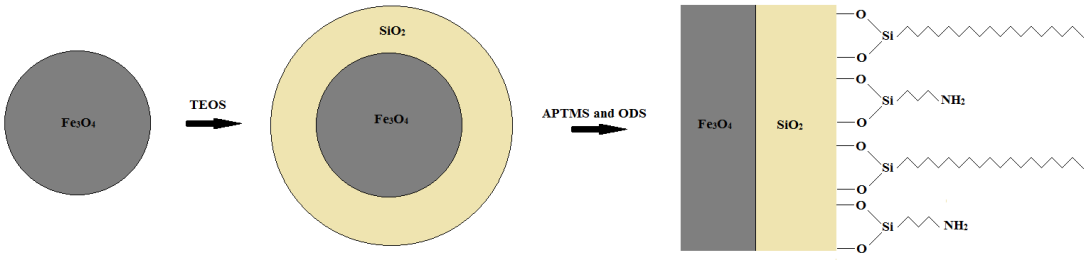

Figure 2: *The overall reaction scheme of the synthesis, coating and amino-functionalization*

2.2.Nanoparticle characterization

2.2.1. X-ray diffraction

X-ray diffraction (XRD) was used to determine the structure of the core of the synthesized nanoparticles and to estimate the particle size by the Scherrer equation [29]. Dried samples were grinded into a fine grain powder, and transferred into a sample container before being analyzed with an X-ray diffractometer (D8 Advance DaVinci, Bruker) for a time period of 30 min at a constant slit width.

2.2.2. Gas adsorption

The Brunauer, Emmett, and Teller (BET) method was used to estimate the specific surface area of the synthesized nanoparticles in three parallels for each sample. The samples were weighed and degassed. The degassing was carried out at 300 °C and about 200 mTorr for 24 hours. After that, the samples were cooled to room temperature and inserted into sample ports of the TriStar 3000 instrument (Micrometics Instrument Corporation). Nitrogen adsorption isotherms were measured at 77 K. The BET equation was used to calculate the specific surface areas [30].

2.2.3. Fourier transform infrared spectroscopy

A Fourier transform infrared spectroscopy (FTIR) analysis was carried out on the nanoparticles produced at the different synthesis stages, as well as for the commercial Isolute NH2 particles. Spectra were recorded between 500 to 4000 cm^{-1} with a Tensor 27 IR spectrophotometer (Bruker, UK) using OPUS software.

2.2.4. Elemental analysis

Elemental analysis was carried out on the unmodified and amino-functionalized nanoparticles. The analysis was performed by the laboratory SGS Multilab (Evry, France). Carbon (C), hydrogen (H) and nitrogen (N) concentrations were determined by thermal conductivity, and oxygen (O) and sulfur (S) by infrared measurements.

The grafting degrees of the ODS and APTMS trimethoxylanes were calculated based on the elemental analysis data. The molar ratio of APTMS to nitrogen is one to one. Assuming that all the nitrogen from the elemental analysis comes from APTMS, mole of APTMS per gram, can be calculated from the relation in equation 1:

$$n_{APTMS} = n_N \tag{1}$$

where n_{APTMS} is the number of mole of APTMS per gram of nanoparticles and n_N is the number of moles of nitrogen per gram of nanoparticles.

The different reaction possibilities of trimethoxysilanes with the silica surface are illustrated in Figure 3, where k is the number of alkoxy groups not reacted with the silica surface. This means that the amount of carbon from one ODS or one APTMS molecule will differ depending on the k value.

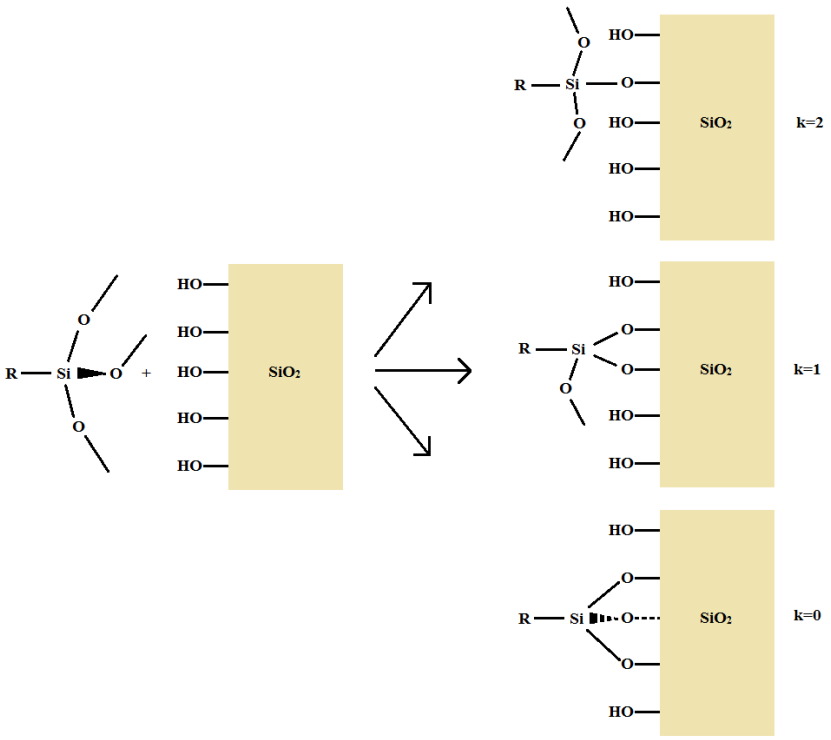

Figure 3: *Reaction possibilities of trimethoxysilanes*

Assuming that all the carbon from the elemental analysis is coming from APTMS and ODS, the number if moles of ODS per gram of nanoparticles can be calculated from equation 2:

$$n_{ODS} = \frac{(n_C - n_{C-APTMS})}{C_{InODS}} = \frac{(n_C - n_N(3+k))}{(18+2k)} \qquad (2)$$

where n_{ODS} is the number of moles of ODS per gram of nanoparticles, C_{InODS} is the number of carbons in ODS reacted onto the surface, n_C is the number of moles of carbon per gram of nanoparticles, $n_{C\text{-}APTMS}$ is the number of moles of carbon per gram coming from the APTMS molecule, and k is the number of alkoxy groups reacted with the silica surface, $k \in [0\text{-}2]$, assuming that k is the same for APTMS and ODS.

The total carbon to nitrogen molar ratio for the functionalized nanoparticles are 3.78 and 4.19 for the toluene and xylene reactions respectively. There are six carbons in unreacted APTMS: three in the chain and one in each of the methoxy groups. With a carbon to nitrogen ratio less than four and assuming that all the carbon in the elemental analysis comes from ODS or APTMS, at least some of the APTMS molecules are totally grafted onto the surface or in a polymerization

reaction. At such low carbon to nitrogen ratio, little carbon is left to account for the ODS, which indicated that the grafting of ODS occurred to a far lesser degree than APTMS. Assuming that all the hydrogen from the elemental analysis comes from APTMS, ODS and unreacted hydroxyl groups on the silica surfaces, the number of unreacted hydroxyl groups can be found from equation 3:

$$n_H - n_{APTMS}(8+3k) - n_{ODS}(37+k) = n_{-OHur} \tag{3}$$

where n_H is number of moles of hydrogen per gram of nanoparticles and n_{-OHur} is number of moles of unreacted hydroxyl groups per gram nanoparticles.

Knowing the specific surface area of the molecules, the number of moles per surface area can be found from equation 4:

$$\frac{Specific\ mole}{Specific\ surface\ area} = \frac{mole}{area} \tag{4}$$

2.2.5. Transmission electron microscopy

Transmission electron microscopy (TEM) was used to estimate size, shape, coating thickness, and flocculation tendency of the nanoparticles. The imaging was carried out on a JEOL JEM-2100F instrument with a field emission gun (FEG) operated at 200kV at the NORTEM TEM Gemini Centre, Norwegian University of Science and Technology (NTNU).

A theoretical specific surface area can be calculated from equations 5 and 6 using the average particle sizes from the TEM images (assuming spherical particles).

$$S_{Fe} = \frac{4\pi r_{Fe}^2}{\rho_{Fe}\frac{4}{3}\pi r_{Fe}^3} = \frac{3}{\rho_{Fe}\, r_{Fe}} \tag{5}$$

$$S_{Si} = \frac{3r_{Si}^{\ 2}}{\rho_{Fe}r_{Fe}^{\ 3} + \rho_{Si}(r_{Si}^{\ 3} - r_{Fe}^{\ 3})} \tag{6}$$

where ρ_{Fe} is the density of iron oxide (5.17 g/mL), ρ_{Si} is the density of silica (2.65 g/mL), r_{Fe} is the average radius for the Fe_3O_4 particles (10 nm), r_{Si} is the average radius for the Fe_3O_4/SiO_2 particles (19 nm), S_{FeT} is the theoretical specific surface area for Fe_3O_4 nanoparticles and S_{SiT} is the theoretical specific surface area for Fe_3O_4/SiO_2 nanoparticles.

2.3.Testing

2.3.1. Selectivity of Isolate NH_2 particles towards naphthenic acid adsorption

Commercial Isolute NH_2 silica particles were used to evaluate the adsorption selectivity of amino groups towards NA in the real crude oil. It was assumed that the particles are 100 % selective towards the NA. The amount of particles needed to adsorb all the NA from the crude oil was calculated based on the particle exchange capacity (PEC) and the measured TAN value, using equation 7.

$$\frac{TAN}{PEC} = \frac{1.7}{0.51}\frac{mg_{KOH}\,g_{particles}}{g_{Oil}\,mmole_{adsorbant}} = \frac{1.7}{0.51*56.1}\frac{g_{particles}}{g_{Oil}} = 0.059 \qquad (7)$$

To eliminate potential contamination, the particles were rinsed in hexane for 24 hours, and dried in nitrogen. The particles (16.19 g) were then added to the crude oil (251.72 g) and shaken for 24 hours, before being removed by centrifugation (11000 rpm, 10 min). The crude oil was examined before and after contact with Isolute NH_2 particles with respect to TAN [25], asphaltene content [24], UV-vis spectroscopy [31], elemental analysis, and FTIR spectroscopy. All the tests were performed using three parallels.

2.3.2. Quartz crystal microbalance

The Quartz crystal microbalance (QCM) method was used to evaluate adsorption of the model NA onto amino functionalized silica surfaces. The experiments were performed with a Q-sense E1 quartz crystal microbalance with simultaneous frequency and dissipation monitoring, mounted with a sensor crystal (Q-Sense Sensor QSX 303 SiO2) with a top layer of silica. The silica sensors were functionalized with amino groups according to the previously described procedure (2.1.4. using toluene) to mimic surfaces of the functionalized Fe_3O_4/SiO_2 NH_2/C_{18} nanoparticles. A stable baseline of a solvent (octane) was established before injecting a continuous flow of NA in octane

solution. After the frequency shift stabilized on the QCM-D, pure octane was washed over the crystal to ensure that the material was properly adsorbed. All surfaces were cleaned according to a standard protocol for silica surface before use. All QCM experiments were performed at 20 °C. A low dissipation (<1E-6) indicated a stiff monolayer adsorption, and the Sauerbrey equation (8) can be used directly to calculate the adsorbed mass:

$$\Delta f = -\frac{2 f_0^2}{\rho_Q \upsilon_Q} \frac{\Delta m}{A} \qquad (8)$$

where Δf is the frequency change, f_0 is the resonance frequency, ρq is the crystal density, υq is the shear velocity of the crystal, Δm is the change in mass and A is the area of the crystal.

2.3.3. Adsorption of model naphthenic acid

The functionalized Fe_3O_4/SiO_2 NH_2/C_{18} and silica-coated Fe_3O_4/SiO_2 magnetic nanoparticles were dried at 60 °C in nitrogen atmosphere for about 24 hours and then washed in octane for another 24 hours under stirring. They were then dried, weighed and made ready for adsorption of the HBA acid from the model solution. The model NA varied in concentration from 0.01 to 1.9 g/L in octane. The nanoparticles were suspended in the model solutions and left under stirring for 24 hours. UV-vis measurements at wavelength 242 nm were used to determine the equilibrium concentrations of the model NA after removal of the nanoparticles. The instrument used for the measurement was UV-2401PC Spectrophotometer (Shimadzu).

3. RESULTS AND DISCUSSION

3.1. Characterization of the synthesized nanoparticles

The diffraction profiles of the synthesized Fe_3O_4 samples and an iron (III) oxide reference sample are presented in Figure 4. There was a major correspondence between the nanoparticles and the reference patterns, confirming that the nanoparticle core composition is consistent with a magnetite structure.

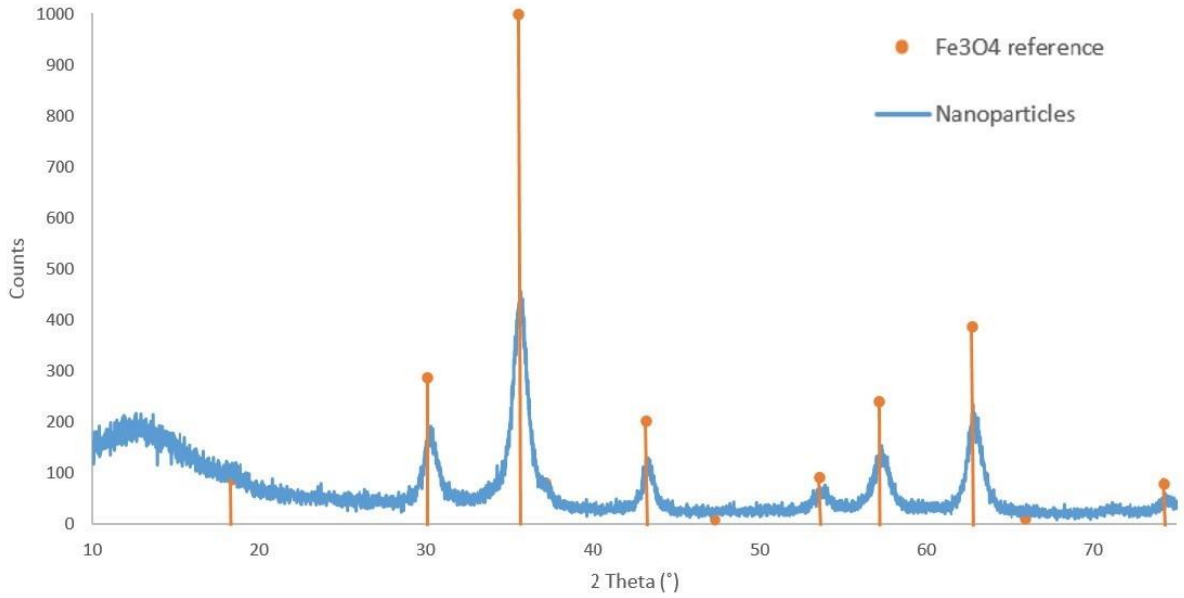

Figure 4: *XRD patterns of synthesized nanoparticles (blue) and iron (III) (orange) oxide*

The average nanoparticle size was estimated to 12 nm with the Scherrers equation, which corresponded to a surface area of approximately 98 m^2/g (assuming spherical nanoparticles).

The BET specific surface areas at the different stages of the nanoparticle synthesis are presented in Table 2. All the synthesized nanoparticle types had similar values within standard deviation. This means that the surface area of the nanoparticles were not significantly affected by the silica coating or the functionalization of the nanoparticles.

Table 2. *Specific surface area of the synthesized nanoparticles*

Nanoparticles	Specific surface area (m^2/g)
Fe_3O_4	100 ± 2
Fe_3O_4/SiO_2	114 ±11
Fe_3O_4/SiO_2 NH_2/C_{18} (xylene reaction)	87 ± 17

Fe_3O_4/SiO_2 NH_2/C_{18} (toluene reaction)	94 ±7

Based on the results and assuming that the nanoparticles were perfect spheres with density of Fe_3O_4 nanoparticles equal to 5.17 g/cm^3 [32], approximated the average size to be 11.7 nm. Both the estimated nanoparticle size and measured surface area corresponded well with the XRD analysis. The nanoparticle diameter increased as a result of silica coating and a decrease in the surface area would be expected. In reality, a slight increase in the surface area is observed, which could be due to an increase in the surface roughness of the nanoparticles.

The FTIR spectra of the synthesized Fe_3O_4, Fe_3O_4/SiO_2 and $Fe_3O_4/SiO_2NH_2/C_{18}$ nanoparticles and the commercial Isolute NH_2 particles are shown in Figure 5.

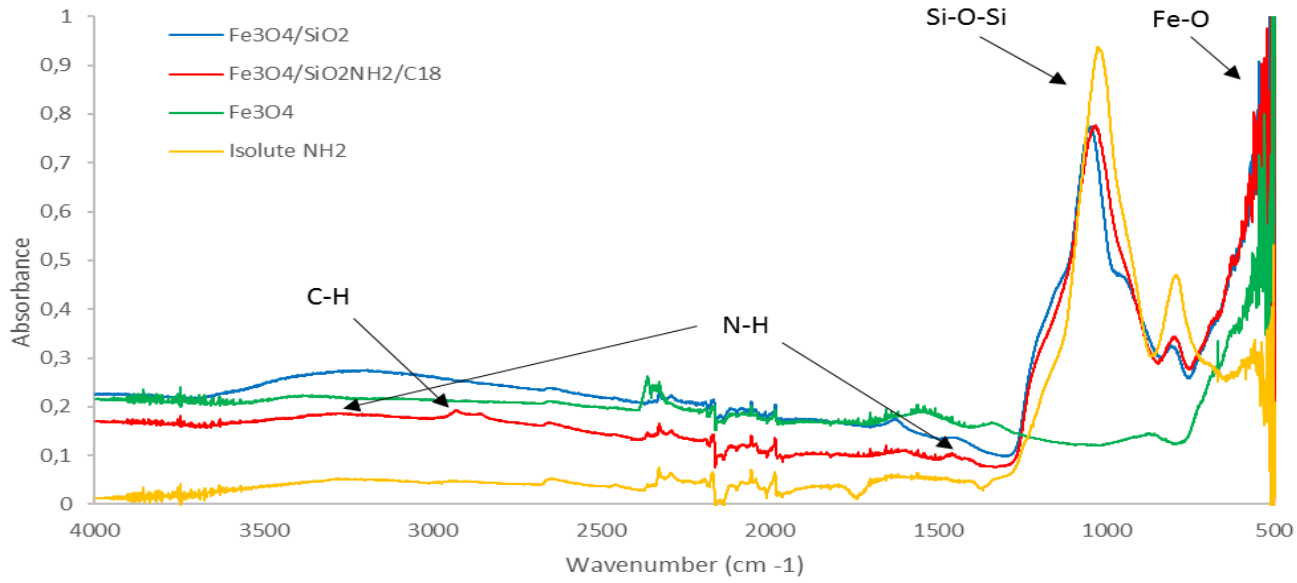

Figure 5: *FTIR spectra of the synthesized nanoparticles and commercial Isolute NH_2 particles*

The peak at 560 cm^{-1} indicates that the Fe-O group is present in all the samples except for the commercial non-magnetic Isolute NH_2 particles. There is a clear indication at 1080 cm^{-1} that Si-O-Si bonds have been formed in the silica coating reaction and that these are also present in the commercial particles. The peaks at 2851 and 2921 cm^{-1} in the amino-functionalized samples may indicate the presence of C-H bonding, and that the C_{18} chains have successfully been grafted onto

the silica surface. The amino groups are expected to be in the 1498 and 3361 cm^{-1} regions, where weak adsorptions can be observed.

The elemental composition analysis results for the Fe_3O_4 and $Fe_3O_4/SiO_2NH_2/C_{18}$ nanoparticles from toluene and xylene reactions are summarized in Table 3.

Table 3: *Elemental analysis values in moles per 100 g of particle*

Element	Fe_3O_4 (g)	Fe_3O_4/SiO_2 NH_2/C_{18} (toluene) (g)	Fe_3O_4/SiO_2 NH_2/C_{18} (xylene) (g)
Hydrogen (H)	0.51	1.03	0.97
Carbon (C)	0.00	0.30	0.27
Nitrogen (N)	0.00	0.08	0.06
Oxygen (O)	1.65	0.97	0.94
Sulfur (S)	0.00	0.00	0.00

The grafting degrees of the ODS and APTMS trimethoxysilanes were estimated based on values obtained through the elemental analysis. The grafting degrees for the APTMS and ODS were calculated to be in the range from 7.31 to 8.41×10^{-24} mole/nm^2 and from 0 to 4.8×10^{-25} mole/nm^2 respectively, showing that it is possible that no ODS has been grafted onto the silica surface (equation 4). The number of unreacted OH groups was calculated to vary from 1.36 to 3.54 $\times10^{-25}$ mole/nm^2.

TEM images of the nanoparticles at different resolutions are presented in Figure 8. The nanoparticles seem to have parallelepiped or octagonal shapes and a tendency to flocculate. Parallel lines in the particles can be observed from Figure 6 (A) indicating the lattices of the atomic structure and that the nanoparticles are most probably monocrystals. The different directions of the parallel lines in the individual nanoparticles is due to the differences in the orientation of the nanoparticles.

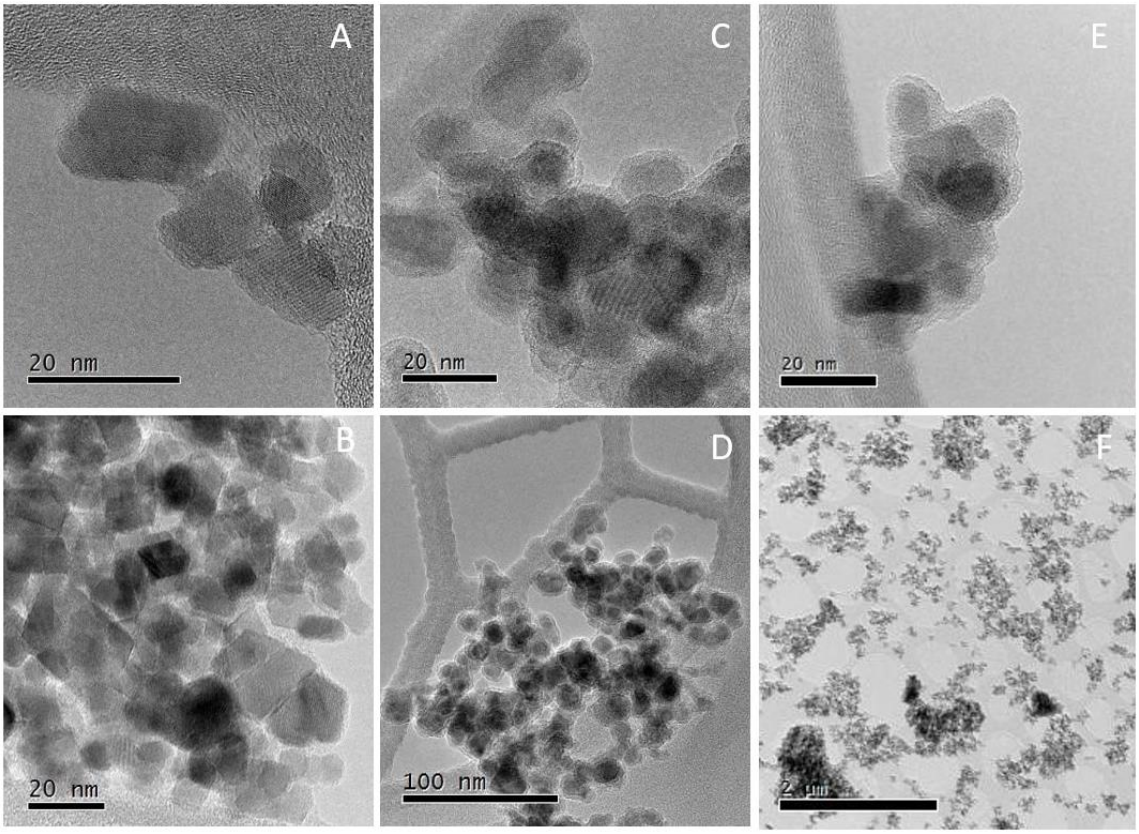

Figure 6: *TEM images of Fe_3O_4 (A, B), Fe_3O_4/SiO_2 (C, D) and $Fe_3O_4/SiO_2NH_2/C_{18}$ (E, F) nanoparticles*

The size of the Fe_3O_4 nanoparticles seems to be in the range from 10 to 30 nm. This compares well to the BET and XRD results. Since sphere is the shape at smallest area to volume ratio, it is expected that the parallelepiped or octagonal shapes would be bigger with the same specific surface area. A typical core-shell structure can be observed from Figure 6 (C and E) for the silica coated Fe_3O_4/SiO_2 nanoparticles. The coating seems to have an amorphous structure. According to the images, the functionalization of the Fe_3O_4/SiO_2 nanoparticles did not result in change of morphology or dispersibility of the nanoparticles.

The images clearly show the nanoparticle morphology and permitted estimation of the nanoparticle size distributions. Average nanoparticle sizes were calculated from the corresponding distributions for the nanoparticles before and after application of the silica coating, and resulted in the average values of 10 and 19 nm, respectively. This indicates that the thickness of the silica coating might be in the range of 4.5 nm. That corresponds well with the value of 4.15 nm calculated from the added amount of TEOS.

The theoretical specific surface area calculated from the size given by the TEM images were 116 m^2/g and 104 m^2/g for Fe_3O_4 and Fe_3O_4/SiO_2 nanoparticles, respectively. This is higher than the measured specific area for Fe_3O_4 from the BET analysis (99 m^2/g). The differences are covered by the standard deviation of the size estimations, but may also be due to the actual nanoparticle size being smaller and because the nanoparticle clusters may block adsorption in the center of the cluster. The theoretical specific surface area calculated for the Fe_3O_4/SiO_2 nanoparticles is slightly lower than the measured specific area from BET analysis (114 m^2/g).

Magnetic properties of the synthesized nanoparticles were evaluated by application of magnetic field (a strong magnet was placed under a flask containing nanoparticle suspension in HCl suspension). The technique confirmed effective magnetic separation of the silica-coated nanoparticles as the liquid phase was clear after a time period of 70 seconds (Fig. 7).

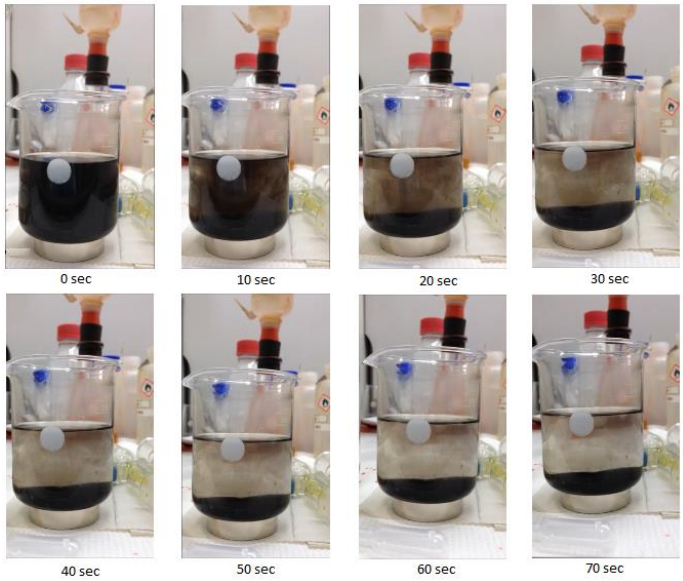

Figure 7: *Nanoparticle separation under magnetic field*

The magnetic properties of the nanoparticles play an important role for the removal of NA responsible for the complexation of metals and can be done according to the principle shown in Figure 8. The specifically functionalized magnetic nanoparticles are dispersed in the model or crude oil phase leading to the surface adsorption of NA. By application of external magnetic field, the NA-coated nanoparticles are removed from the medium. After an appropriate treatment, the

NA are desorbed from the nanoparticles, and the latter can be recovered and recycled for new extractions.

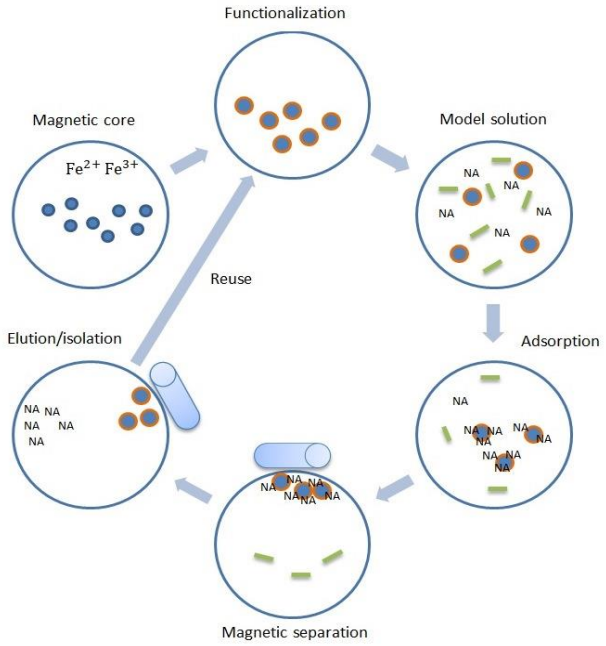

Figure 8: *The proposed scheme of nanoparticle application for extraction of NA*

3.2.Selectivity of Isolute NH2 particles towards naphthenic acid adsorption

The adsorption selectivity of Isolute NH_2 particles towards NA present in a real crude oil was evaluated to verify that no other crude oil components were removed during the adsorption process.

The average TAN values of crude oil before and after the adsorption was measured to be 1.70 and 0.13 mg KOH/g_{oil} respectively, giving a reduction of 92.2 %. This confirmed that a major part of the acidic components/NA in the crude oil was removed. The results of the elemental analysis before and after adsorption are presented in Table 4.

Table 4. *Concentrations of elements in crude oil*

Element	Before adsorption (wt%)	After adsorption (wt%)	Relative change (%)
Carbon (C)	86.3	86.7	0.46
Oxygen (O)	0.39	0.28	-28.2

Hydrogen (H)	12.66	12.8	1.11
Sulfur (S)	0.39	0.39	0.00
Nitrogen (N)	0.09	0.08	0.01

It is well established that the asphaltenes and resins in crude oils often contain the major part of the nitrogen, oxygen and sulfur [33]. No significant changes in concentrations of carbon, hydrogen, and sulfur were registered here. However, the concentration of oxygen was reduced by 28.2 %. This reduction could be attributed to removal of the carboxyl groups of NA, which is consistent with reduction in TAN.

The asphaltenes present in crude oils are generally comprised of acidic and basic components [34-36]. So-called acidic asphaltenes contain acidic groups and may, therefore, be partly removed from crude oil together with the NA. The crude oil used in this study has a low asphaltene content of 0.5 wt%. A slight reduction by 0.1 wt% in asphaltene concentration was registered as a result of the crude oil treatment with the Isolute NH_2 particles. The UV-vis spectroscopy was used to conclusively evaluate possible removal of asphaltenes by the particles (Fig. 9). The results revealed superimposed curves for the crude oil before and after the adsorption in the ultraviolet and visible spectra regions confirming that no asphaltenes were adsorbed [37].

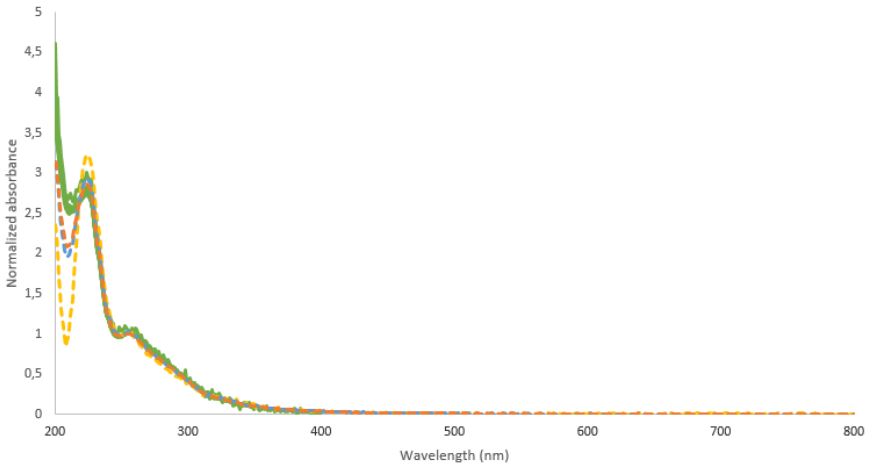

Figure 9: *Normalized absorbance spectra at 256 nm (solid lines correspond to the spectra before adsorption, while the dashed lines correspond to the spectra after adsorption)*

FTIR was used to evaluate possible changes in concentrations of the crude oil components. A summary of functional groups which can be identified in the FTIR spectra is given in Table 5 [38].

Table 5. *Functional groups from the crude oil IR spectra*

Peak	Wavelength (cm^{-1})	Mode of vibration	Functional group
P1 and P2	729 and 813	C-H bending	CH of substituted benzene
P3	1378	C-H sym. def.	$-CH_2$ of saturate
P4	1459	C-H deformation	$-CH_2$ and $-CH_3$ of saturate
P5	2854	C-H stretching	$-CH_2$ and $-CH_3$ of saturate
P6	2921	C-H stretching	$-CH_2$ and $-CH_3$ of saturate

The recorded spectra for the crude oil treated by amino-functionalized particles are presented in Figure 10. The structure seems to be preserved as no major changes of the CH bonding or other functions were observed.

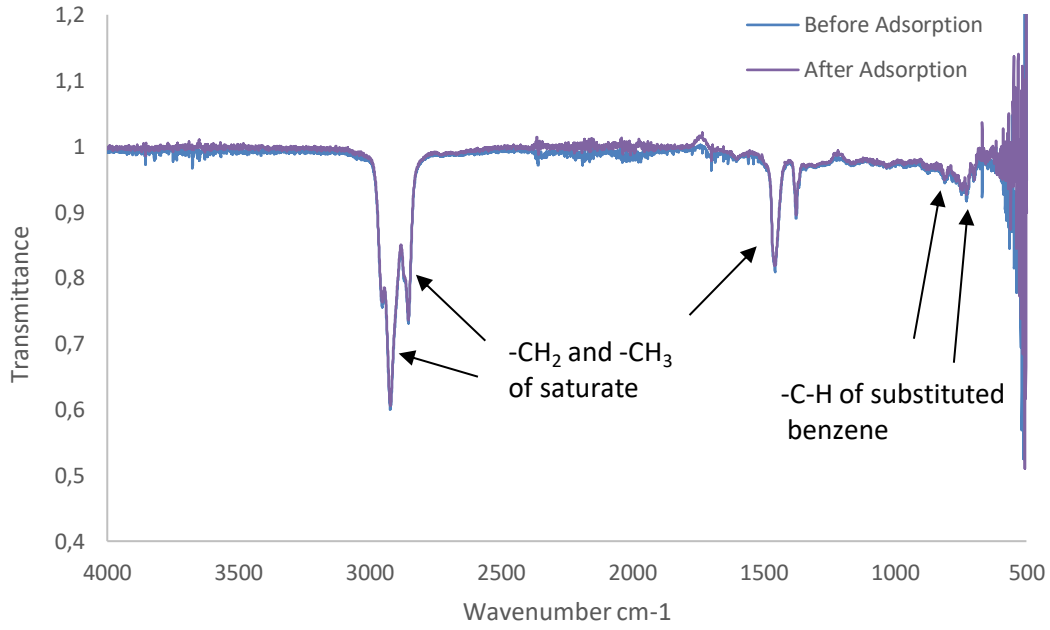

Figure 10: *FTIR spectra of crude oil before (blue line) and after (yellow line) treatment with Isolute NH_2 particles*

The performed tests verified that no other crude oil compounds are removed during the adsorption procedure and confirmed selectivity of amino groups towards NA present in the crude oil.

3.3. Adsorption of model NA onto functionalized QCM surface

The goal with the QCM experiments was to register a real-time adsorption of the model NA (HBA) onto the surfaces of interest and provide a qualitative evaluation of the adsorption process. The QCM experiments were also performed on unmodified silica plates for comparison. The amount of reagents, ODS and APTMS, used here was the same as in the original synthesis, but it has to be noted that the reaction surfaces for the sensors and the nanoparticles are different.

Figure 11 shows the change in frequency and dissipation over time. The 3rd overtone frequency change and dissipation change was plotted for both the unmodified and modified surfaces. From 0 to 300 seconds pure octane is present in the QCM chamber with no flow. At 300 seconds a flow (0.5 mL/min) of 500 ppm HBA in octane starts. At 600 seconds the flow stops, and the octane flow (0.5 mL/min) starts.

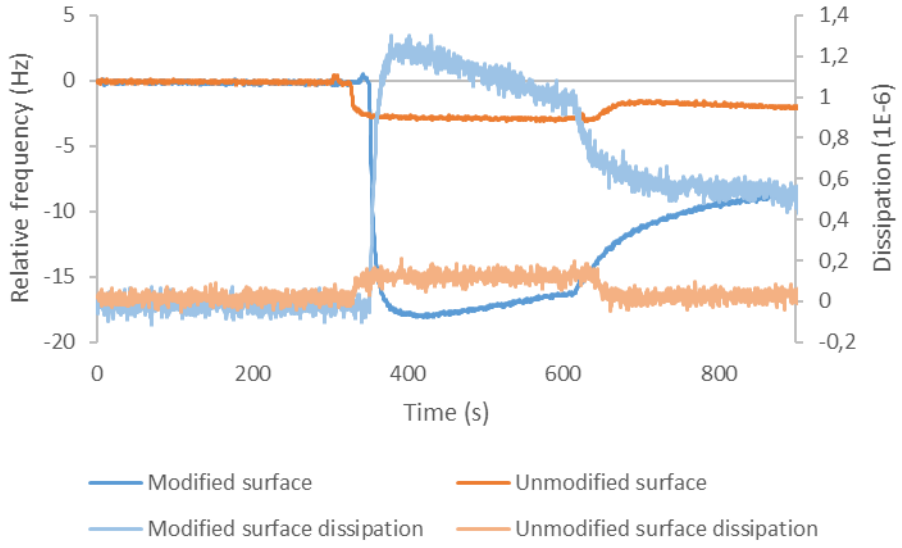

Figure 11: *Change in frequency and dissipation over time for unmodified and amino-functionalized silica surfaces*

Since the dissipation is low (smaller than 10^{-6}), it can be assumed that the adsorption layer is a rigid layer. The Sauerbrey equation (Eq. 8), can therefore be applied for obtaining surface concentration over time. The adsorption capacity of the modified sensors compared to the unmodified was found to be about 4.1 times higher. It can also be seen that the adsorption is very rapid, and that when the saturated surface is exposed to pure solvent (after 600 s) some of the adsorbed material desorbs indicating that the adsorption is not irreversible.

Height of the adsorbed layer can be calculated from the surface concentration and density of the adsorbed layer. An estimation of 1.01 g/mL was used. The height of the adsorbed layer can give an indication of the orientation of adsorbed molecule relative to the surface, knowing the length of the adsorbed molecule (Fig. 12).

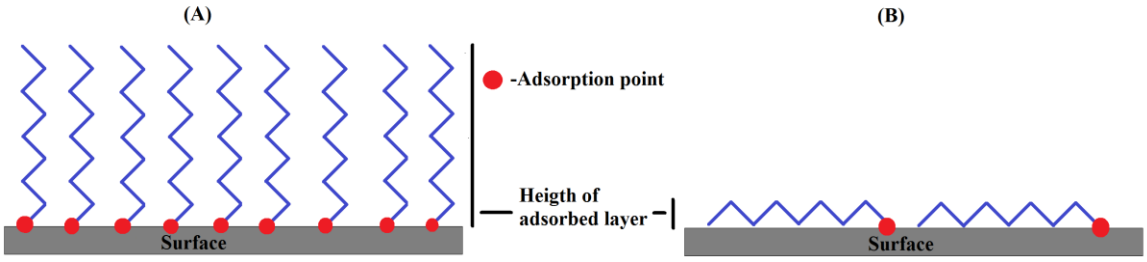

Figure 12: *Illustration of molecule tail orientation as a function of height of the adsorbed layer. (A) Max height for adsorbed monolayer, molecules are orthogonal to the adsorbed surface. (B) Adsorbed molecules are parallel to the surface.*

An estimation of the maximum length of HBA molecule can be found using a bond length for C-C of 1.5 Å, a bond angle of 109.5° and 11 C-C bonds in HBA molecule. The length of the HBA was estimated to be 1.6 nm. Table 6 summarizes the estimated heights of adsorbed HBA layers at the nanoparticle and sensor surfaces. All heights of the adsorbed layers were estimated to be smaller than the maximum length of HBA molecule, with the largest value registered for the modified QCM sensor.

Table 6: *Height of the adsorbed layers for the different surfaces*

Surface	Height adsorbed layer (nm)
Modified QCM sensor	1.48
Unmodified QCM sensor	0.36

Functionalized particles UV-vis	0.85
Silica coated particles UV-vis	1.31

3.4. Adsorption of model NA onto functionalized nanoparticles

The adsorption isotherms for the Fe_3O_4/SiO_2 and $Fe_3O_4/SiO_2NH_2/C_{18}$ nanoparticles are given in Figure 13. HBA dissolved in octane was used as a model system mimicking real crude oil containing indigenous NA.

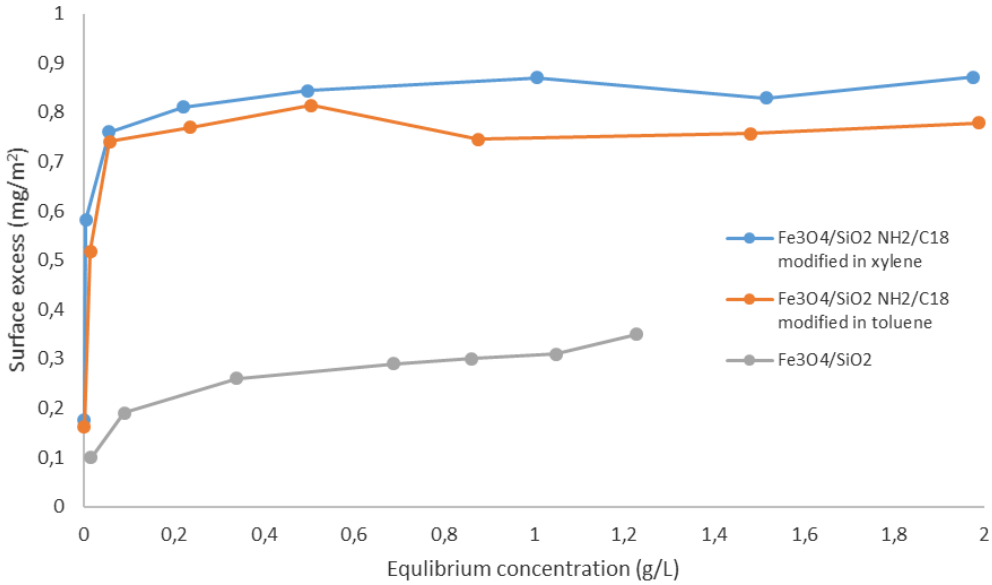

Figure 13: *Adsorption isotherms for Fe_3O_4/SiO_2 and $Fe_3O_4/SiO_2NH_2/C_{18}$ nanoparticles*

The results confirmed that the amino-functionalization modification of the nanoparticles increased the adsorption of acid. The two functionalization methods revealed similar results for the adsorption of model NA onto the nanoparticle surface. The amino-functionalized $Fe_3O_4/SiO_2NH_2/C_{18}$ nanoparticles displayed 2.7 times higher adsorption capacity compared to the unmodified silica-coated Fe_3O_4/SiO_2 samples. According to the QCM-D data, adsorption capacity of the modified sensors compared to the unmodified sensor differed by a somewhat higher factor of 4.1. The lower value for the nanoparticles may be due to a lesser degree of amino group coverage. It was calculated that the surface concentration at the end of the QCM-D experiment was 1.5 mg/m^2 and 0.37 mg/m^2 for the modified and unmodified surfaces, respectively. The

surface concentration from the adsorption measured with UV-vis was 0.31 mg/m^2 and 0.85 mg/m^2 for Fe_3O_4/SiO_2 and Fe_3O_4/SiO_2 NH_2/C_{18} nanoparticles, respectively. The reason for the lower values in the latter measurement may be that all the adsorbed molecules have been measured in the QCM experiment, while the UV-spectroscopy only determined the HBA surface concentration.

CONCLUSIONS

Adsorption selectivity of amino groups towards NA present in the crude oil was confirmed by adsorption experiments with commercial Isolute NH_2 particles. Magnetic iron oxide silica-coated Fe_3O_4/SiO_2 and amino-functionalized Fe_3O_4/SiO_2 NH_2/C_{18} nanoparticles were designed and tested for adsorption of HBA dissolved in octane. The Fe_3O_4/SiO_2 NH_2/C_{18} nanoparticles were obtained by two different methods, a high-pressure autoclave experiment with toluene as solvent and a newly developed reflux experiment using xylene. The Fe_3O_4/SiO_2 and Fe_3O_4/SiO_2 NH_2/C_{18} nanoparticles were compared by their efficiency to adsorb the HBA, and tested with respect to various parameters. Both types of the nanoparticles exhibited magnetic properties. The specific surface area of the synthesized nanoparticles was estimated by means of BET, XRD, and TEM. The Fe_3O_4/SiO_2 nanoparticles showed a specific surface area of 114 m^2/g, while slightly less was registered for the Fe_3O_4/SiO_2 NH_2/C_{18} samples, 86.9 m^2/g. and 94.2 m^2/g for the nanoparticles modified in xylene and toluene, respectively. Elemental analysis revealed that APTMS groups were successfully grafted onto the surface and that ODS had been grafted to a lesser degree or not at all. TEM confirmed presence of the magnetic core and silica coating of the separate nanoparticles as well as nanoparticle agglomerates. The average nanoparticle/coating sizes were calculated from a size distribution analysis of the TEM images. The average size for the unmodified Fe_3O_4 nanoparticles was 10 nm, while thickness of the silica coating was estimated to be ca. 4.5 nm for the Fe_3O_4/SiO_2 nanoparticles. The Fe_3O_4/SiO_2 NH_2/C_{18} nanoparticles showed about 2.7 times higher adsorption capacity compared to the Fe_3O_4/SiO_2 nanoparticles. Model QCM-D experiments with a flat silica surface showed a strong, fast adsorption of the model acid onto the surface, with a large increase for the modified silica surface. These experiments also showed that the adsorption is probably reversible. Both functionalization methods for nanoparticles showed similar acid adsorption results and can potentially be used for grafting of amino groups onto nanoparticle silica surfaces.

AUTHOR INFORMATION

Corresponding Author

* Tel: +47 41018485; e-mail: galinanorge@gmail.com

ACKNOWLEDGMENT

The authors acknowledge the financial support from VISTA – a basic research program in collaboration between The Norwegian Academy of Science and Letters, and Equinor. Mia Ronander is thanked for performing with the XRD tests.

REFERENCES

1. Meredith, W., Kelland, S. J., Jones, D. M., *Influence of Biodegradation on Crude Oil Acidity and Carboxylic Acid Composition.* Org. Geochem, 2000. **31**(11): p. 1059-1073.
2. Qian, K., Robbins, W. K., Hughey, C. A., Cooper, H. J., Rodgers, R. P., Marshall, A. G., *Resolution and Identification of Elemental Compositions for More than 3000 Crude Acids in Heavy Petroleum by Negative-Ion Microelectrospray High-Field Fourier Transform Ion Cyclotron Resonance Mass Spectrometry.* Energy Fuels, 2001. **15**(6): p. 1505-1511.
3. Slavcheva, E., Shone, B., Turnbull, A., *Review of Naphthenic Acid Corrosion in Oil Refining.* Br. Corros. J., 1999. **34**: p. 125-131.
4. Clemente, J.S.F., P. M., *A Review of the Occurrence, Analyses, Toxicity, and Biodegradation of Naphthenic Acids.* Chemosphere, 2005. **60**(5): p. 585-600.
5. Baugh, T.D., Wolf, N. O., Mediaas, H., Vindstad, J. E., Grande, K., *Characterization of a Calcium Naphthanate Deposit - The ARN Acid Discovery.* Prepr. - Am. Chem. Soc., Div. Pet. Chem., 2004. **49**(3): p. 274-276.
6. Loh, W., Mohamed, R.S., and Ramos, A.C.S., *Aggregation of asphaltenes obtained from a Brazilian crude oil in aromatic solvents.* Pet Sci Technol, 1999. **17**(1-2): p. 147-163.
7. Brandal, O., Hanneseth, A.-M. D., Hemmingsen, P. V., Sjoblom, J., Kim, S., Rodgers, R. P., Marshall, A. G., *Isolation and Characterization of Naphthenic Acids from a Metal Naphthenate Deposit: Molecular Properties at Oil-Water and Air-Water Interfaces.* J. Dispersion Sci. Technol., 2006. **27**(3): p. 295 - 305.
8. Zhang, A., Ma, Q., Wang, K., Liu, X., Shuler, P., Tang, Y., *Naphthenic acid removal from crude oil through catalytic decarboxylation on magnesium oxide.* Applied Catalysis A: General, 2006. **303**: p. 103-109.
9. Lutnaes, B.F., Brandal, Ø., Sjöblom, J., Krane, J., *Archaeal C80 isoprenoid tetraacids responsible for naphthenate deposition in crude oil processing.* Organic and Biomolecular Chemistry, 2006. **4**(4): p. 616-620.

10. Taylor, S.E., and Chu, H.T., *Metal Ion Interactions with Crude Oil Components: Specificity of Ca2+ Binding to Naphthenic Acid at an Oil/Water Interface.* Colloids Interfaces, 2018. **2**(40).
11. Dahl Hanneseth, A.-M., Selsbak, C. and Sjöblom, J., *Behavior and Stability of Naphthenic Acid/Naphthenate Stabilized Emulsions. Mixed C80-Tetraacid and Stearic Acid Stabilization.* Journal of Dispersion Science and Technology, 2010. **31**: p. 770-779.
12. Williams, H., Dyer, S., Graham, G. M. . *Understanding the Factors Influencing the Formation and Control of Calcium Naphthenate Solids and Stabilised Emulsions Using a Novel Laboratory Flow Rig*. in *International Symposium on Oilfield Chemistry*. 2007. Houston, Texas, U.S.A.
13. Vindstad, J.E., Bye, A.S., Grande, K.V., Hustad, B.M., Hustvedt , E., Nergård, B., *Fighting Naphthenate Deposition at the Heidrun Field*, in *International Symposium on Oilfield Scale*. 2003, Society of Petroleum Engineers: Aberdeen, United Kingdom.
14. Goldszal, A., Hurtevent, C., Rousseau, G., *Scale and Naphthenate Inhibition in Deep-Offshore Fields*, in *International Symposium on Oilfield Scale*. 2002, Society of Petroleum Engineers: Aberdeen, United Kingdom.
15. Rousseau, G., Zhou, H., Hurtevent, C., *Calcium Carbonate and Naphthenate Mixed Scale in Deep-Offshore Fields*, in *International Symposium on Oilfield Scale*. 2001: Aberdeen, United Kingdom.
16. Hurtevent, C., Ubbels, S., *Preventing naphthenate stabilised emulsions and naphthenate deposits on fields producing acidic crude oils*, in *SPE Eighth International Symposium on Oilfield Scale*. 2006: Aberdeen, United kingdom. p. 69-75.
17. Wang, X., Shi, Y., Graff, R.W., Lee, D., Gao, H., *Developing recyclable pH-responsive magnetic nanoparticles for oil-water separation.* Polymer, 2015. **72**: p. 361-367.
18. Davidson, A., Huh, C., Bryant, S.L., *Focused Magnetic Heating Utilizing Superparamagnetic Nanoparticles for Improved Oil Production Applications*, in *SPE International Oilfield Nanotechnology Conference and Exhibition*. 2012, Society of Petroleum Engineers: Noordwijk, The Netherlands.
19. Atta, A.M., Al-Lohedan, H.A., and Al-Hussain, S.A., *Functionalization of Magnetite Nanoparticles as Oil Spill Collector.* Int. J. Mol. Sci. 2015, 2015. **16**: p. 6911-6931.
20. Ko, S., Kim , E.S., Park , S., Daigle , H., Milner, T.E., Huh, C., Bennetzen, M.V., Geremia, G.A., *Oil Droplet Removal from Produced Water Using Nanoparticles and Their Magnetic Separation*, in *SPE Annual Technical Conference and Exhibition*. 2016, Society of Petroleum Engineers: Dubai, UAE.
21. Simonsen, G., Strand, M., Øye, G., *Potential applications of magnetic nanoparticles within separation in the petroleum industry.* Journal of Petroleum Science and Engineering, 2018(165).
22. Lu, A.-H.S., E.L.; Schuth, F., *Magnetic Nanoparticles: Synthesis, Protection, Functionalization, and Application.* Angewandte Chemie International Edition, 2007. **46**: p. 1222-1244.
23. Bohara, R.A., Thorat, N.D., and Pawar, S.H., *Role of functionalization: strategies to explore potential nano-bio applications of magnetic nanoparticles.* RSC Advances, 2016. **6**(50): p. 43989-44012.
24. Hannisdal, A., Hemmingsen, P.V. and Sjöblom, J., *Group-Type Analysis of Heavy Crude Oils Using Vibrational Spectroscopy in Combination with Multivariate Analysis.* Ind. Eng. Chem. Res., 2005. **44**(5): p. 1349-1357.

25. *Standard Test Method for Acid Number of Petroleum Products by Potentiometric Titration*
26. Zhang C, W.B., Morgenstern B, Zentgraf H, Eisenhut M, Untenecker H, Kru¨ger R, Huss R, Seliger C, Semmler W, Kiessling F *Silica- and Alkoxysilane-Coated Ultrasmall Superparamagnetic Iron Oxide Particles: A Promising Tool To Label Cells for Magnetic Resonance Imaging.* Langmuir, 2007. **23**: p. 1427-1434.
27. Deng Y-H, W.C.-C., Hu J-H, Yang W-L, Fu S-K *Investigation of formation of silica-coated magnetite nanoparticles via sol–gel approach.* Colloids and Surfaces A: Physicochem. Eng. Aspects 2005. **262**: p. 87–93.
28. Zhang, X., Niua, H., Pana, Y., Shia, Y., Cai, Y., *Modifying the surface of Fe3O4/SiO2 magnetic nanoparticles with C18/NH2 mixed group to get an efficient sorbent for anionic organic pollutants.* Journal of Colloid and Interface Science, 2011. **362**(1): p. 107–112.
29. Patterson, A.L., *The Scherrer Formula for X-Ray Particle Size Determination.* Phys. Rev. , 1939. **56**(10): p. 978-982.
30. Brunauer, S., Emmett, P.H., Teller, E., *Adsorption of Gases in Multimolecular Layers.* J. Amer. Chem. Soc., 1938. **60**(2): p. 309-319.
31. Banda-Cruz, E.E., Padrón-Ortega, S.I., Gallardo-Rivas, N.V., Rivera-Armenta, J.L., Páramo-García, U., Díaz Zavala, N.P. and Mendoza-Martínez, A.M., *Crude oil UV spectroscopy and light scattering characterization.* Pet Sci Technol, 2016. **34**: p. 732-738.
32. Blaney, L., *Magnetite (Fe3O4): Properties, Synthesis, and Applications.* Lehigh University Preserve, 2007. **15**: p. Paper 5.
33. Sjöblom, J., Simon, S., Xu, Z., *Model molecules mimicking asphaltenes.* Advances in Colloid and Interface Science, 2015. **218**: p. 1-16.
34. Hosseinpour, N., Khodadadi, A.A., Bahramian, A., Mortazavi, Y., *Asphaltene adsorption onto acidic/basic metal oxide nanoparticles toward in situ upgrading of reservoir oils by nanotechnology.* Langmuir, 2013. **29**(46): p. 14135-46.
35. Peng, J., Tang, G.Q., Kovscek, A.R., *Oil chemistry and its impact on heavy oil solution gas drive.* Journal of Petroleum Science and Engineering, 2009. **66**(1-2): p. 47-59.
36. Simon, S., Nenningstand, A.L., Herschbach, E., Sjoblom, J., *Extraction of basic components from petroleum crude oil.* Energy and Fuels, 2010. **24**: p. 1043-50.
37. Alboudwarej, H., Jakher, R.K., Svrcek, W.Y. and Yarranton, H.W., *Spectrophotometric Measurement of Asphaltene Concentration.* Petroleum Science and Technology, 2004. **22**(5 and 6): p. 647-664.
38. Adedosu, T.A.a.S., O.O., *Characterization of Niger Delta Crude Oil by Infrared Spectroscopy.* Journal of Applied Sciences, 2005. **5**(5): p. 906-909.